

Simultaneous reception of both quadratures of 40-Gb/s DQPSK using a simple monolithic demodulator

C. R. Doerr, D. M. Gill, A. H. Gnauck, L. L. Buhl, P. J. Winzer, M. A. Cappuzzo, A. Wong-Foy, E. Y. Chen, and L. T. Gomez

Lucent Technologies, Bell Laboratories, 791 Holmdel-Keyport Road, Holmdel, NJ 07733
crdoerr@lucent.com

Abstract: We demonstrate a novel device that demodulates both quadratures of the optical differential quadrature phase shift keying (DQPSK) format in a single interferometer. We present simultaneous measurements of both DQPSK quadratures at 42.7-Gb/s.

©2005 Optical Society of America

OCIS codes: (060.2330) Fiber optics communications; (130.3120) Integrated optics devices

1. Introduction

The differential quadrature phase-shift keying (DQPSK) format uses four phase levels to transmit data. Single-polarization demonstrations have been done at 10 Gb/s^[1,2], 20 Gb/s^[3,4,5], 40 Gb/s^[6], and 80 Gb/s^[7]. Similar to differential phase shift keying (DPSK), DQPSK yields a close to 3-dB improved receiver sensitivity in optical signal-to-noise ratio (OSNR) over on/off keying (OOK) at forward-error correction rates, if balanced detection is used^[8]. DQPSK has an additional advantage over conventional binary DPSK in that it has a narrower optical spectrum, which allows for more dispersion (both chromatic and polarization-mode) and for stronger optical filtering. However, a main drawback of DQPSK is that it traditionally requires two Mach-Zehnder delay-line interferometers (MZDIs) with two sets of balanced detectors in the receiver. Also, DQPSK requires a stringent wavelength alignment of the transmitter and MZDI (~ 1 pm for 40 Gb/s)^[9], and thus each MZDI must be tightly feedback-controlled to lock it to the transmitter wavelength. Here we demonstrate a novel device that combines the two MZDIs into a single MZDI with four outputs (1×4 MZDI). Thus we need only one frequency stabilization control loop, and the receiver can be more compact and less expensive.

2. Design

The proposed 1×4 DQPSK demodulator is shown in Figs. 1a and c. It consists of a 1×2 y-branch coupler and a 2×4 star coupler^[10] connected by two waveguides with a path-length difference equal to the group velocity divided by the symbol rate. (The 2×4 star coupler is actually a 4×4 star coupler with the center two ports on one side connected to the interferometer arms.) For comparison, previous DQPSK demodulators (Fig. 1b) consisted of a 3-dB coupler followed by two separate 1×2 MZDIs, each with a 1×2 and 2×2 coupler.

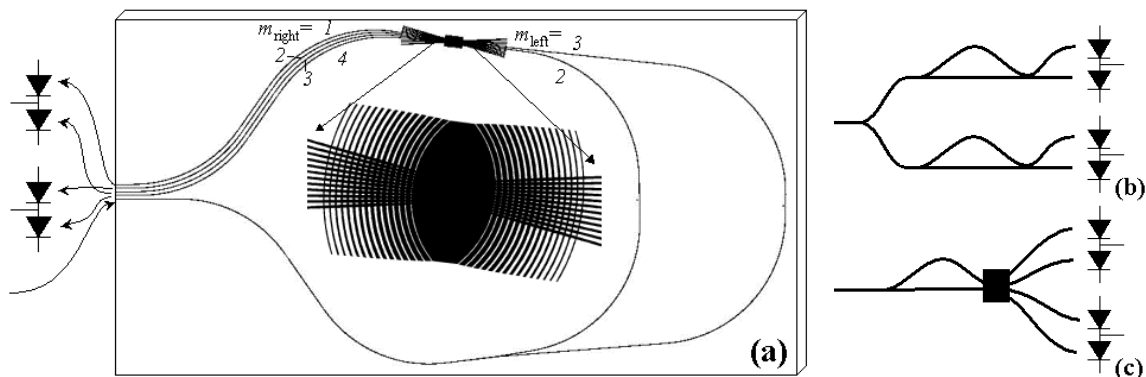


Fig. 1. (a) Waveguide layout of the 1×4 demodulator. Inset shows a detail of the star coupler. One can see the segmentation used to reduce the star coupler loss and loss variation. Chip size is $2.5 \text{ cm} \times 1.2 \text{ cm}$. (b) Schematic of traditional DQPSK demodulator and (c) schematic of proposed DQPSK demodulator.

A physical way to understand the demodulator is the following: in DQPSK the information is encoded in four different levels in the phase difference between adjacent symbols. When the signal first enters the demodulator, it is split in two signals by the y-branch coupler. One of the interferometer arms is one symbol length longer than the other arm. The two signals then recombine in the star coupler. The focal point at the output of the star coupler

depends on the phase difference between the adjacent symbols (see Fig. 2b). If the phase difference between the symbols is 0° , the signal is focused between outputs #2 and #3. This gives a -1 (normalized) from the upper balanced detector and a $+1$ from the lower balanced detector. We will call this $\{-1,+1\}$. If the phase difference is $+90^\circ$, it is focused between outputs #1 and #2, giving $\{+1,+1\}$. If it is -90° , it is focused between outputs #3 and #4, giving $\{-1,-1\}$. Finally, if it is 180° , it is focused at both edges of the star coupler Brillouin zone, with equal power in outputs #1 and #4, giving $\{+1,-1\}$.

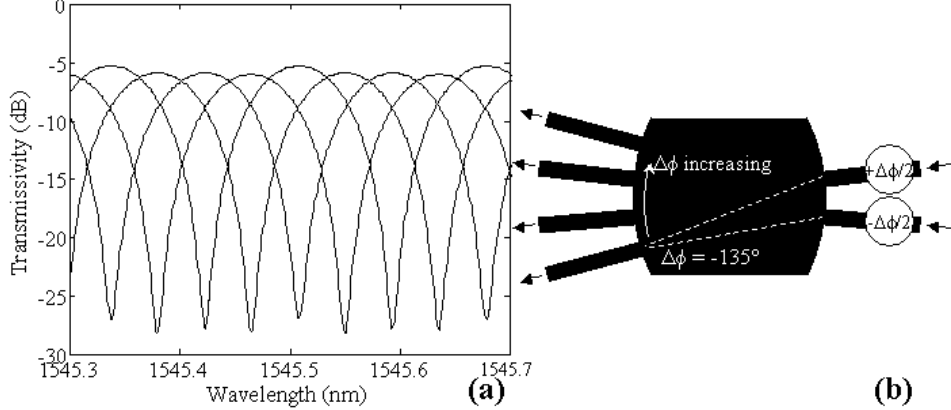


Fig. 2. (a) Measured fiber-to-fiber transmissivity of the input to the four outputs of the demodulator. Averaged over all polarizations. Resolution is 1 pm. (b) Schematic of the 2×4 star coupler operation. The two inputs from the right are the two MZI arms. $\Delta\phi$ represents the phase difference between the two inputs to the star coupler.

A mathematical way to understand the demodulator is the following: the phase acquired by a signal passing from port m_{left} to m_{right} in an ideal $M \times M$ star coupler is

$$\phi_M(m_{\text{left}}, m_{\text{right}}) = \frac{2\pi}{M} \left(m_{\text{left}} - \frac{M+1}{2} \right) \left(m_{\text{right}} - \frac{M+1}{2} \right) \quad (1)$$

neglecting any overall constant phase. As explained above, we use ports $m_{\text{left}} = 2$ and 3 as connected to the interferometer arms, and send ports $m_{\text{right}} = 1$ and 3 to the first balanced receiver and ports $m_{\text{right}} = 2$ and 4 to the second balanced receiver. Using Eq. (1), we find $[\phi_4(2,1) - \phi_4(3,1)] - [\phi_4(2,3) - \phi_4(3,3)] = \pi$, $[\phi_4(2,2) - \phi_4(3,2)] - [\phi_4(2,4) - \phi_4(3,4)] = \pi$, and $[\phi_4(2,1) - \phi_4(3,1)] - [\phi_4(2,2) - \phi_4(3,2)] = \pi/2$, which is what is needed for a DQPSK demodulator.

In an actual star coupler, there are some additional design details. The simplest design is to use a large center-to-center waveguide spacing at the slab region. Then there is negligible mutual coupling. In such a design the phases obey Eq. (1), but the insertion loss and loss imbalance are high (excess loss of ~ 0.5 dB for the center outputs and ~ 2.0 dB for the outer outputs). A better design is to use a relatively small center-to-center waveguide spacing at the slab region, together with segmentation^[11] and converging tapers^[12], to reduce the loss and loss imbalance (excess loss of ~ 0.1 dB for the center outputs and ~ 1.1 dB for the outer outputs, in our case). However, the mutual coupling between waveguides causes aberrations, resulting in Eq. (1) no longer holding true. But by moving the focal points of the two star coupler boundaries into the waveguide array^[13], one can obey Eq. (1) to within $\sim \pm 1^\circ$ while maintaining the reduced loss.

3. Results

The chip was made in 0.80%-index-step, 6.0- μm -thick core, silica-on-silicon waveguides using the waveguide layout of Fig. 1. The time delay between MZI arms is 46.8 ps. The polarization-dependent wavelength (PDW) shift of the fabricated chips is ~ 60 pm, due to strain in the silica. We diced a slot through the center of the two MZI arms and inserted a polyimide half-wave plate. This reduced the PDW shift to ~ 7.5 pm. We attached a fiber ribbon and placed the chip on a thermoelectric cooler. The measured transmissivities from the input to the four outputs are shown in Fig. 2a. The fiber-to-fiber insertion loss ranges from 5.2 to 6.0 dB. As in the traditional DQPSK demodulator, there is an intrinsic 3-dB loss. This is because only two inputs of the 4×4 star coupler are illuminated, making the focal spot on the outputs too large for the waveguides. The variation in loss appears to be mainly due to packaging and connectors, because the loss variation due to the star coupler alone should result in the two center outputs having equal but lower loss than the two outer outputs. The extinction ratio averaged over polarization is ~ 22 dB for all outputs.

We generated a 42.7 Gb/s optical return-to-zero (RZ) DQPSK signal using a pulse carver followed by a nested MZI modulator, as in Ref [6]. Figure 3a shows the experimental setup. The demodulator PDW of 7.5 pm was

enough to cause noticeable polarization dependence, so a polarization controller was used before the demodulator. We have subsequently shown that the PDW can be improved by using a higher performance waveplate. The polarization controller was not adjusted during the data collection.

The inset of Fig. 3b shows the measured electrical eye diagrams from the two sets of balanced detectors. Both sets of balanced detectors were operating simultaneously. The eye diagrams look different mainly because the first and second balanced receiver have differing electrical bandwidths of ~ 40 GHz and ~ 30 GHz, respectively.

Figure 3b shows the measured bit-error rate (BER) vs. OSNR for using either the traditional 1×2 MZDI (square symbols) or the new 1×4 MZDI (circle symbols). The difference in performance is < 0.2 dB. In both cases, BER performance was nearly identical for both quadratures. Importantly, both quadratures were measured *simultaneously* on two separate BER test sets (BERTs) in the 1×4 MZDI case.

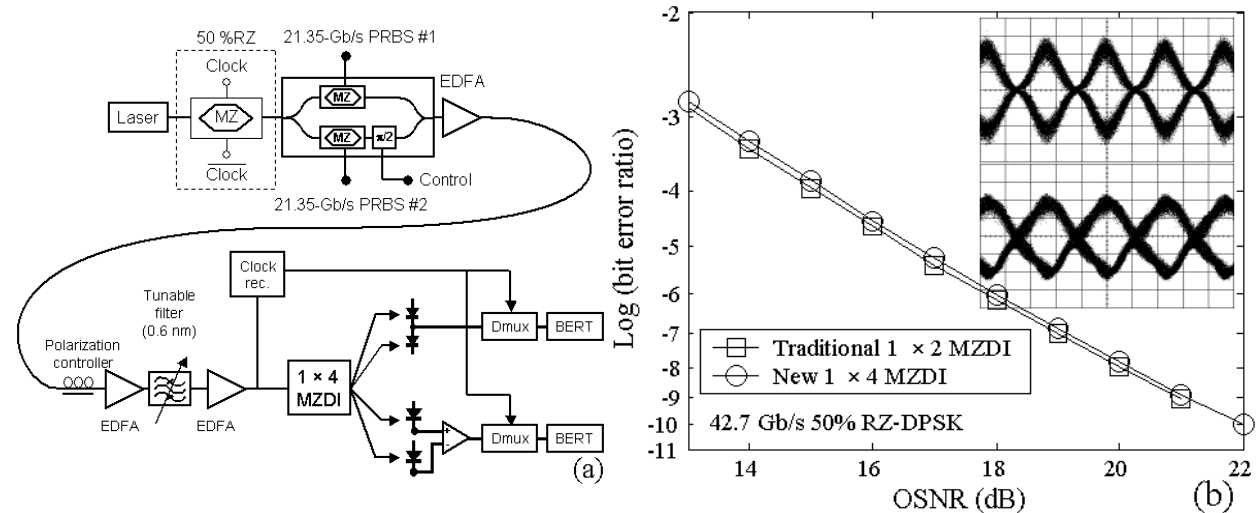


Fig. 3. (a) Experimental setup. The PRBS length is $2^{15}-1$, and the patterns in the two quadratures are shifted by $\sim 2^{14}$ bits. (b) Measured BER vs. OSNR (0.1-nm bandwidth) using a traditional 1×2 MZDI (square markers) and the new 1×4 MZDI (circle markers). In both cases both quadratures were nearly identical, so the results from only one quadrature were plotted for each case. With the 1×4 MZDI, both quadratures were measured simultaneously. The inset in (b) shows the measured electrical eye diagrams from the two sets of balanced detectors.

In summary, we demonstrated a simple device to demodulate both quadratures of optical DQPSK and presented simultaneous demodulation of the complete DQPSK data. The new 1×4 DQPSK demodulator has the advantages of less feedback controls, a smaller total demodulator size, and easier receiver construction.

References

- R. A. Griffin, R. I. Johnstone, R. G. Walker, J. Hall, S. D. Wadsworth, K. Berry, A. C. Carter, M. J. Wale, J. Hughes, P. A. Jerram, and N. J. Parsons, "10 Gb/s optical differential quadrature phase shift key (DQPSK) transmission using GaAs/AlGaAs integration," OFC, PD FD6 (2002).
- T. Tokle, C. R. Davidson, M. Nissov, J.-X. Cai, D. Foursa, and A. Pilipetskii, "6500 km transmission of RZ-DQPSK WDM signals," *Electronics Letters* **40**, pp. 444-445 (2004).
- P. S. Cho, V. S. Grigoryan, Y. A. Godin, A. Salamon, and Y. Achiam, "Transmission of 25-Gb/s RZ-DQPSK signals with 25-GHz channel spacing over 1000 km of SMF-28 Fiber," *IEEE Photon. Technol. Lett.* **15**, 473-475 (2003).
- H. Kim and R.-J. Essiambre, "Transmission of 8×20 Gb/s DQPSK signals over 310-km SMF with 0.8-b/s/Hz spectral efficiency," *IEEE Photon. Technol. Lett.* **15**, 769-771 (2003).
- K. Ishida, K. Shimizu, T. Mizuochi, K. Motoshima, D.-S. Ly-Gagnon, and K. Kikuchi, "Transmission of 20×20 Gb/s RZ-DQPSK signals over 5090 km with 0.53 b/s/Hz spectral efficiency," OFC, FM2 (2004).
- A. H. Gnauck, P. J. Winzer, S. Chandrasekhar, and C. Dorrer, "Spectrally efficient (0.8 b/s/Hz) 1-Tb/s (25×42.7 Gb/s) RZ-DQPSK transmission over 28 100-km SSMF spans with 7 optical add/drops," ECOC, Postdeadline Paper (2004).
- N. Yoshikane and I. Morita, "1.14 b/s/Hz spectrally-efficient 50×85.4 Gb/s transmission over 300 km using copolarized CS-RZ DQPSK signals," OFC, PDP38 (2004).
- G. Kramer, A. Ashikhmin, A. J. van Wijngaarden, and X. Wei, "Spectral efficiency of coded phase-shift keying for fiber-optic communication," *IEEE Journal of Lightwave Technology* **21**, 2438-2445 (2003).
- H. Kim and P. J. Winzer, "Robustness to laser frequency offset in direct-detection DPSK and DQPSK ...," *J. Light. Tech.* **21**, 1887-1891 (2003).
- C. Dragone, "Efficient $N \times N$ star coupler base on Fourier optics," *Electron. Lett.*, **24**, 942-944 (1988).
- Y. P. Li, "Optical device having low insertion loss," U. S. Patent 5 745 618, Apr. 28, 1998.
- C. R. Doerr, R. Pafchek, and L. W. Stulz, "16-band integrated dynamic gain equalization filter with less than 2.8-dB insertion loss," *IEEE Photon. Technol. Lett.* **14**, 334-336 (2002).
- C. Dragone, "An $N \times N$ optical multiplexer using a planar arrangement of two star couplers," *IEEE Photon. Technol. Lett.* **3**, 812-815 (1991).